Spatiotemporal patterns of temperature inversions and impacts on surface PM_{2.5} across China

Yonglin Fang¹, Hancheng Hu¹, Xiangdong Zheng², Jianping Guo³, Xingbing Zhao⁴, Fang Ma⁵, Hao Wu¹

¹College of Electronic Engineering, Chengdu University of Information Technology, Chengdu 610225, China

²Chinese Academy of Meteorological Sciences, Beijing 100081, China

³State Key Laboratory of Severe Weather Meteorological Science and Technology & Specialized Meteorological Support Technology Research Center, Chinese Academy of Meteorological Sciences, Beijing 100081, China

⁴Chengdu Institute of Plateau Meteorology, China Meteorological Administration, Chengdu 610072, China

⁵Yunnan Atmospheric Observation Technology Support Center, Kunming 650034, China

Correspondence: Hao Wu(wuhao@cuit.edu.cn)

This supplementary material includes 10 Figs and 2 Tables.

Fig S1. Site filtering method. (a) Relationship between distance and the number of matching stations. (b) Example diagram of site matching process. 'r' represents the distance from the nearest air quality monitoring station to the sounding station.

Fig S2. Inversion frequency of TI, SBI and EI at BJT 08:00.

Fig S3. Inversion frequency of TI, SBI and EI at BJT 20:00.

Fig S4. Inversion strength of TI, SBI and EI at BJT 08:00.

Fig S5. Inversion strength of TI, SBI and EI at BJT 20:00.

Fig S6. Inversion thickness of TI, SBI and EI at BJT 08:00.

Fig S7. Inversion thickness of TI, SBI and EI at BJT 20:00.

Table S1. Annual Mean Values of Temperature Inversion Parameters by Region at BJT 08:00.

Table S2. Annual Mean Values of Temperature Inversion Parameters by Region at BJT 20:00.

Fig S8. Distribution of PM_{2.5} concentration differences with and without temperature inversion at BJT 08:00.

Fig S9. Distribution of PM_{2.5} concentration differences with and without temperature inversion at BJT 20:00.

Fig S10. Fitting relationship between inversion thickness and PM_{2.5} concentration across seven regions of China from 2016 to 2021.

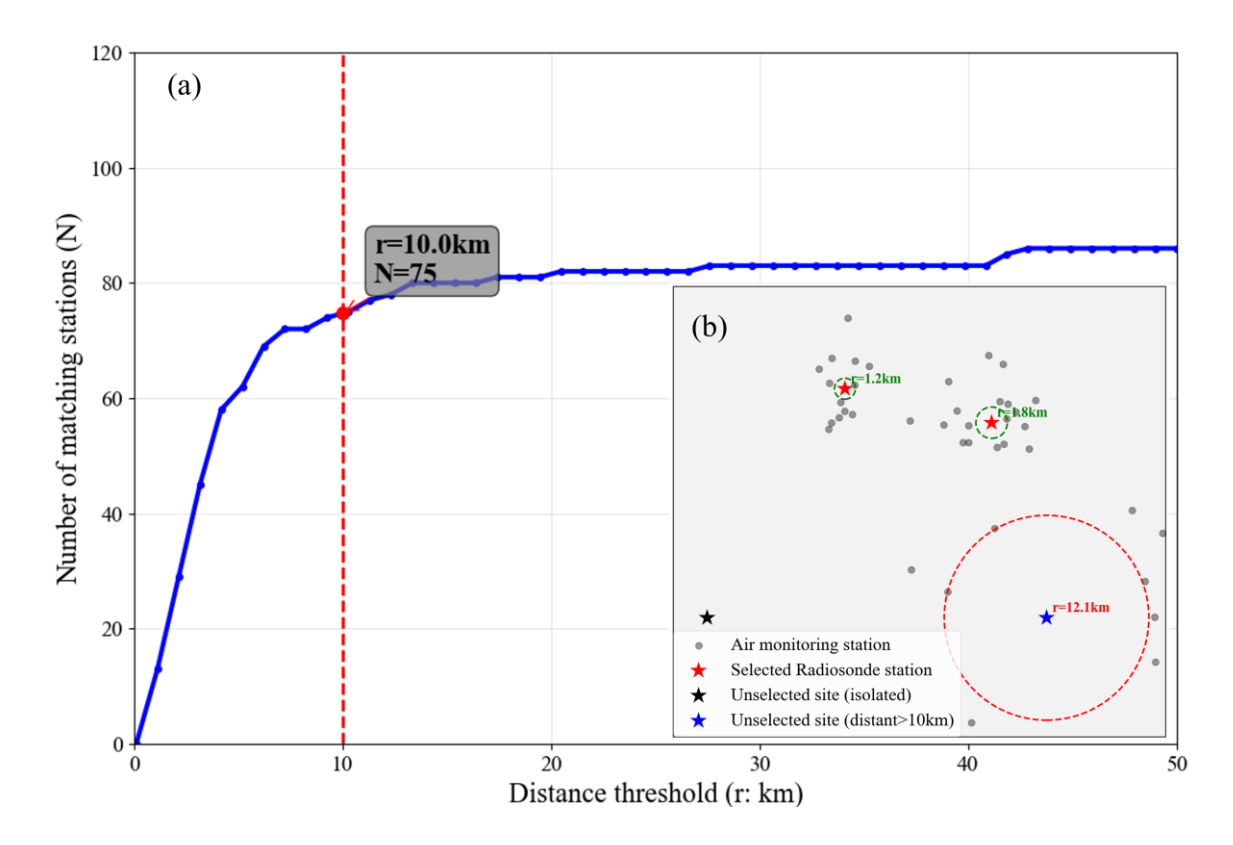


Fig S1. Site filtering method. (a) Relationship between distance and the number of matching stations. (b) Example diagram of site matching process. 'r' represents the distance from the nearest air quality monitoring station to the sounding station.

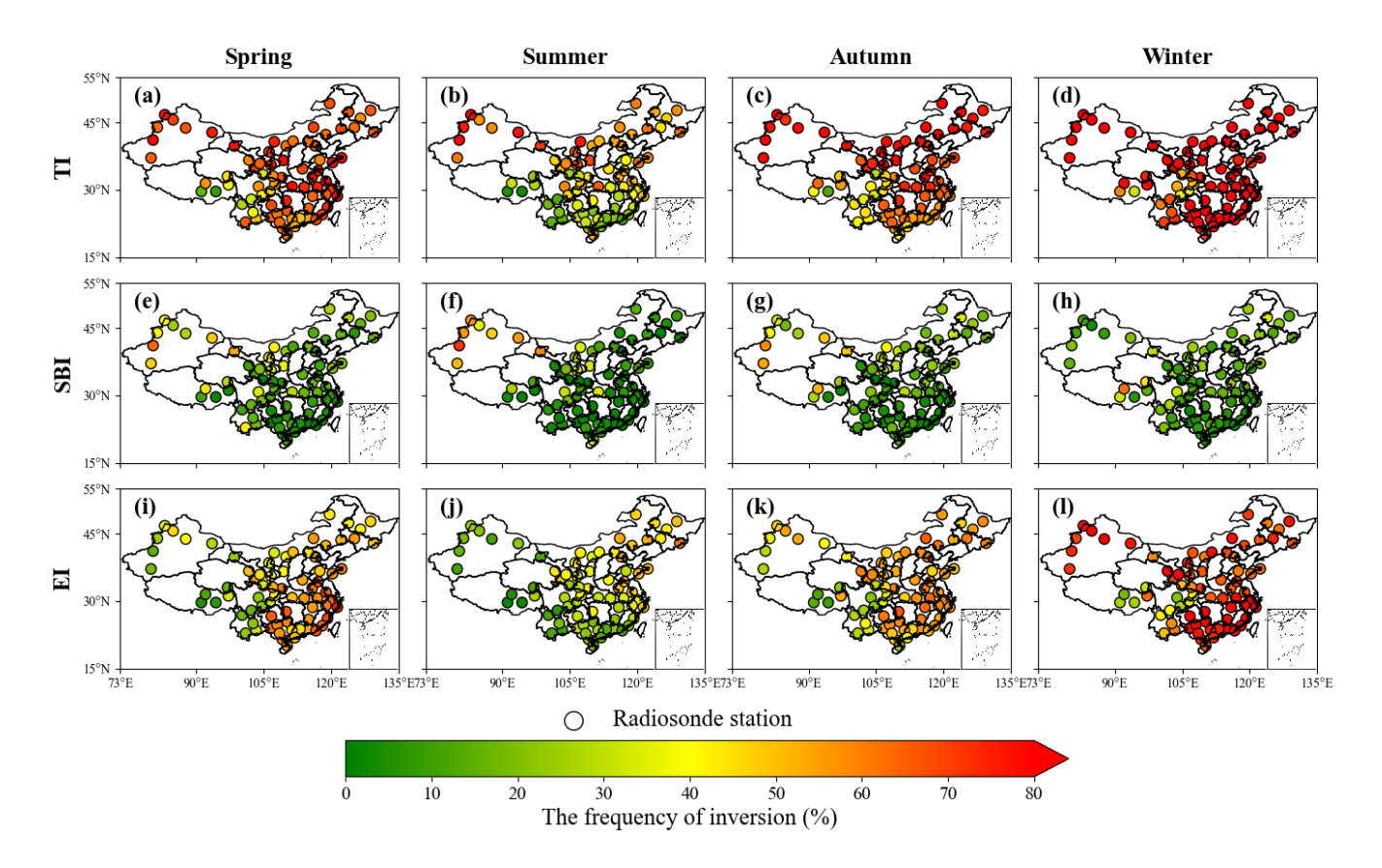


Fig S2. Inversion frequency of TI, SBI and EI at BJT 08:00.

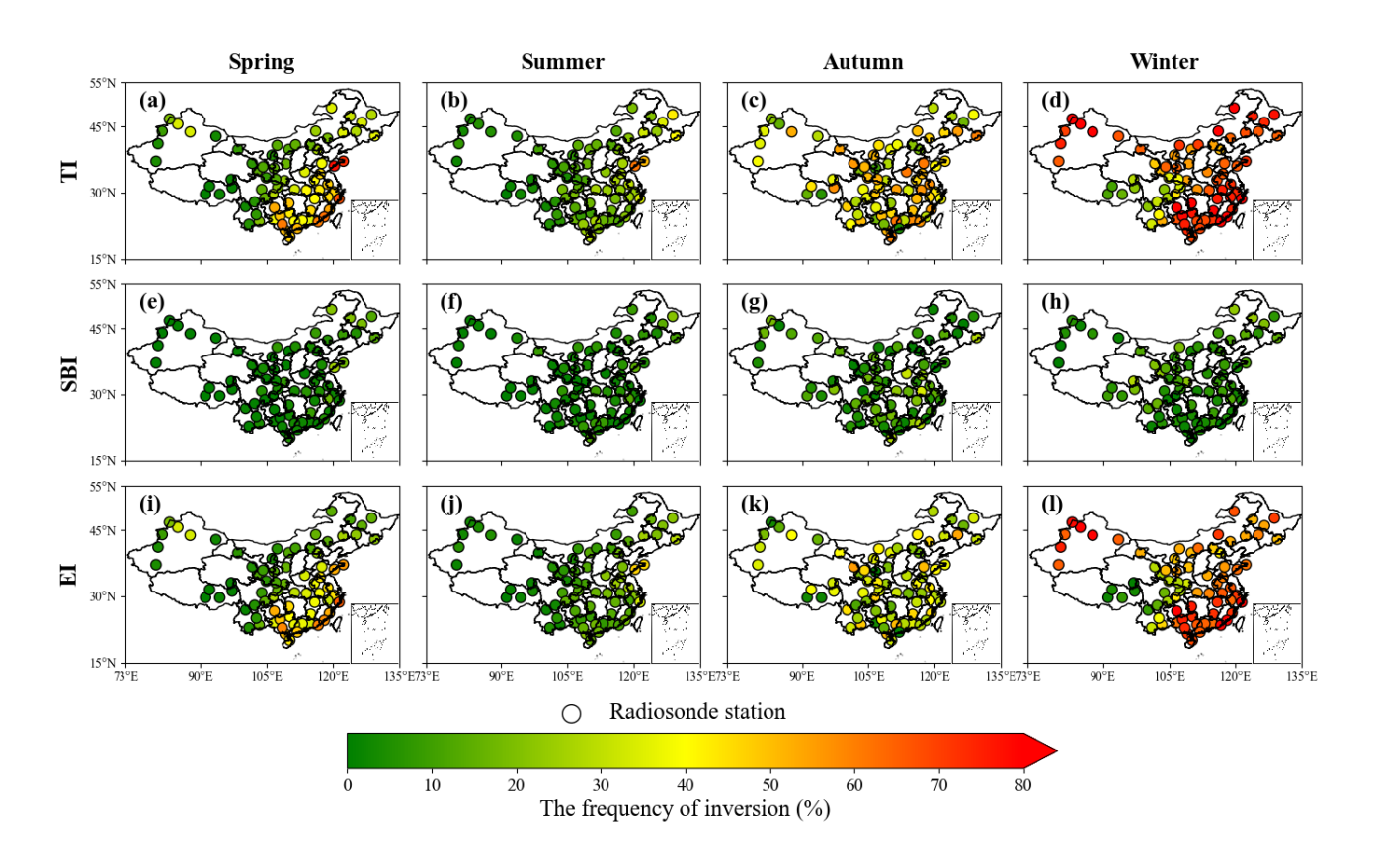


Fig S3. Inversion frequency of TI, SBI and EI at BJT 20:00.

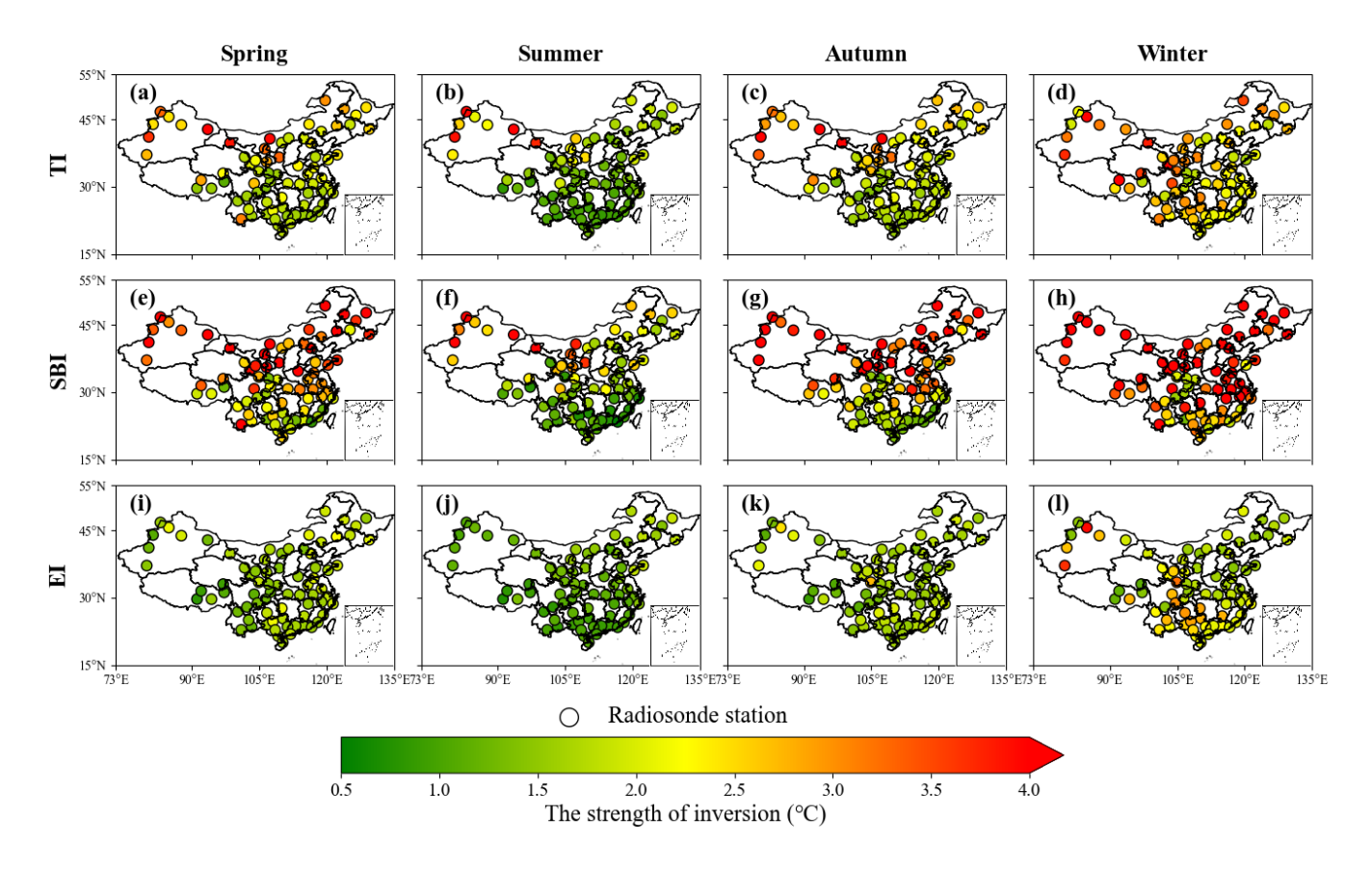


Fig S4. Inversion strength of TI, SBI and EI during at BJT 08:00.

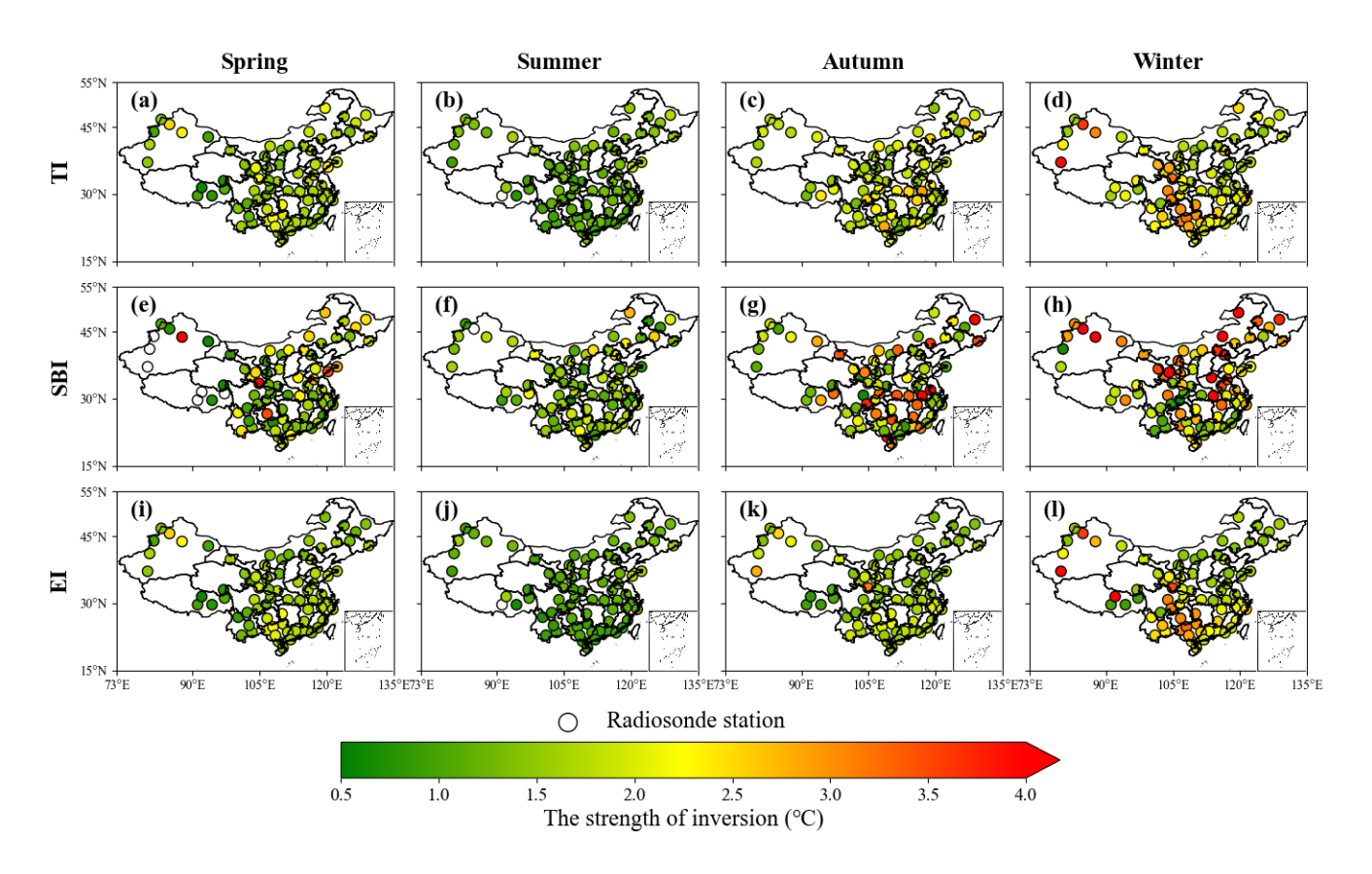


Fig S5. Inversion strength of TI, SBI and EI during at BJT 20:00.

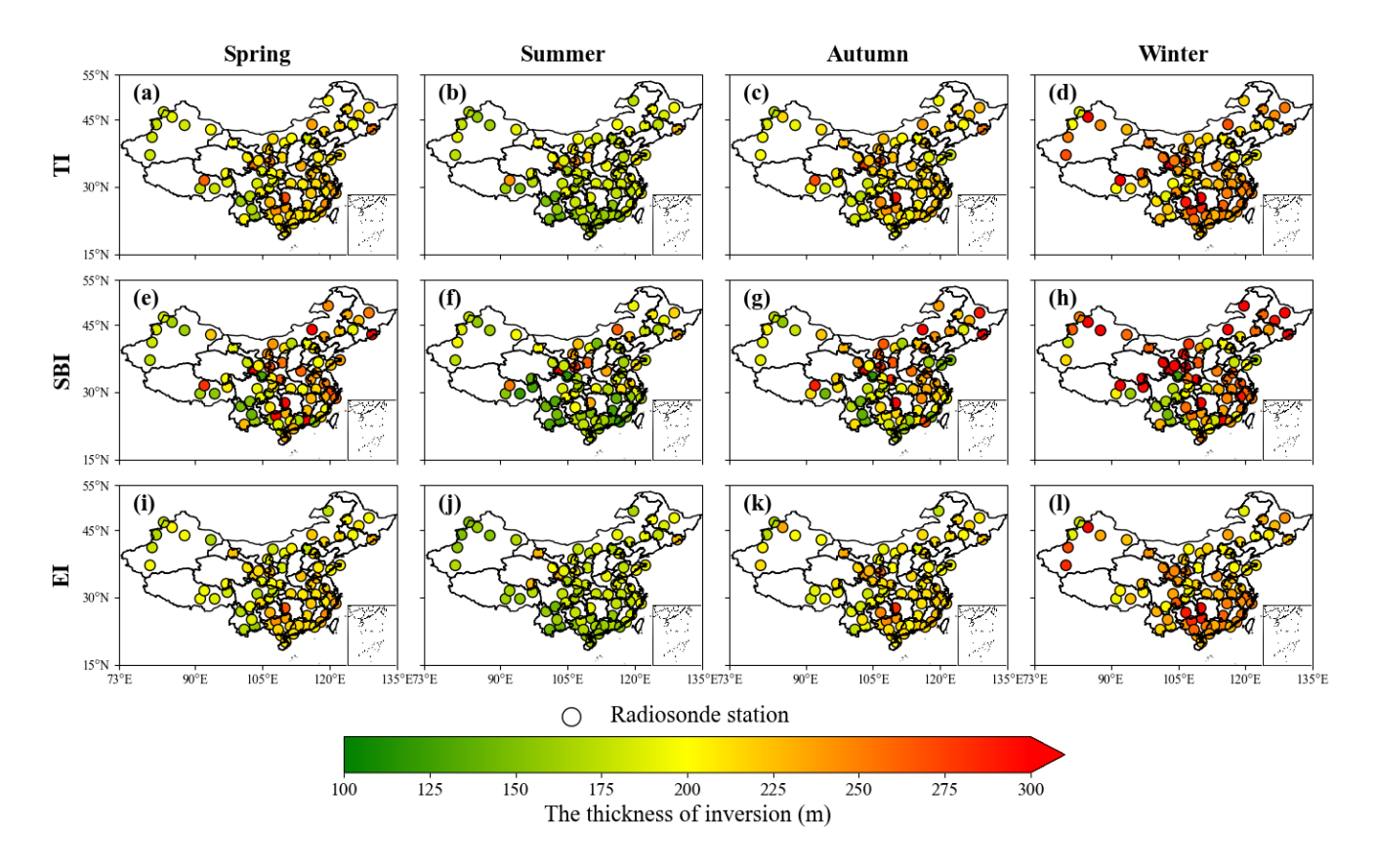


Fig S6. Inversion thickness of TI, SBI and EI during at BJT 08:00.

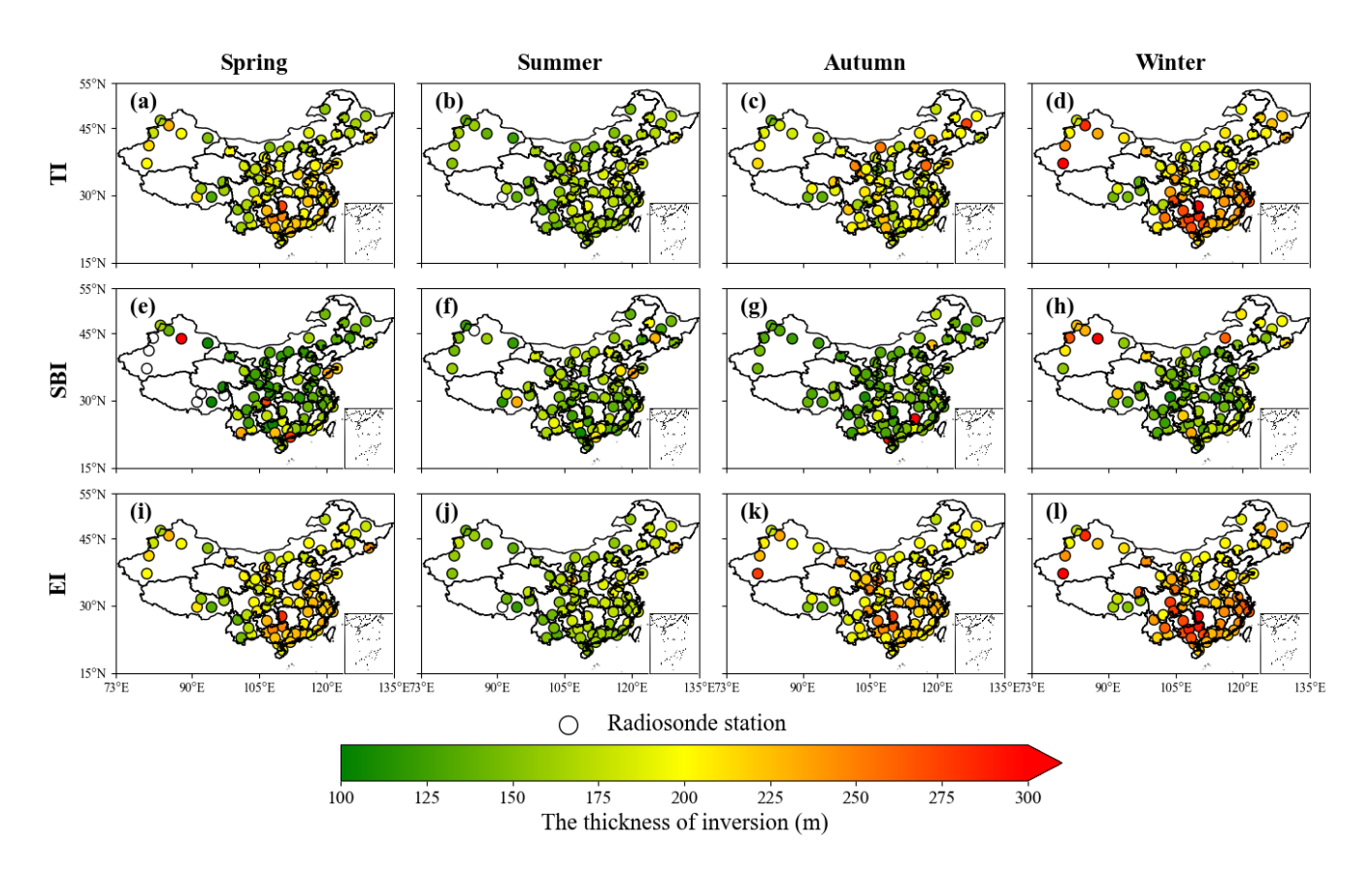


Fig S7. Inversion thickness of TI, SBI and EI during at BJT 20:00.

Table S1. Annual mean values of temperature inversion parameters by region at BJT 08:00.

	TI			SBI			EI		
Region	$F_{TI}(\%)$	Δ <i>T</i> (°C)	$\Delta H(m)$	$F_{SBI}(\%)$	ΔT (°C)	$\Delta H(m)$	$F_{EI}(\%)$	ΔT (°C)	$\Delta H(m)$
Central	70.0	2.16	233	14.5	3.91	249	55.0	1.76	233
East	67.0	1.92	219	9.2	2.84	221	57.8	1.74	219
North	72.6	2.36	210	18.6	4.30	237	54.0	1.68	200
North East	70.7	2.32	223	16.1	4.26	258	54.6	1.71	213
North West	70.5	2.81	219	26.0	4.19	235	44.5	1.86	216
South	56.5	1.87	222	6.1	1.78	204	50.4	1.87	225
South West	43.7	2.07	204	15.0	2.55	196	28.7	1.61	201

Table S2. Annual mean values of temperature inversion parameters by region at BJT 20:00.

		TI			SBI			EI	
Region	$F_{TI}(\%)$	ΔT (°C)	$\Delta H(m)$	$F_{SBI}(\%)$	ΔT (°C)	$\Delta H(m)$	$F_{EI}(\%)$	ΔT (°C)	$\Delta H(m)$
Central	44.4	1.95	228	5.5	2.80	149	38.9	1.85	239
East	51.5	1.79	213	6.3	2.10	161	45.2	1.75	220
North	38.9	1.90	184	11.1	2.80	152	27.8	1.52	196
North East	48.1	1.80	195	15.9	2.39	162	32.2	1.48	210
North West	28.7	2.21	206	5.4	2.88	174	23.3	1.99	218
South	44.6	1.99	224	3.8	1.67	166	40.8	2.02	230
South West	18.9	1.84	186	4.2	1.67	156	14.7	1.76	198

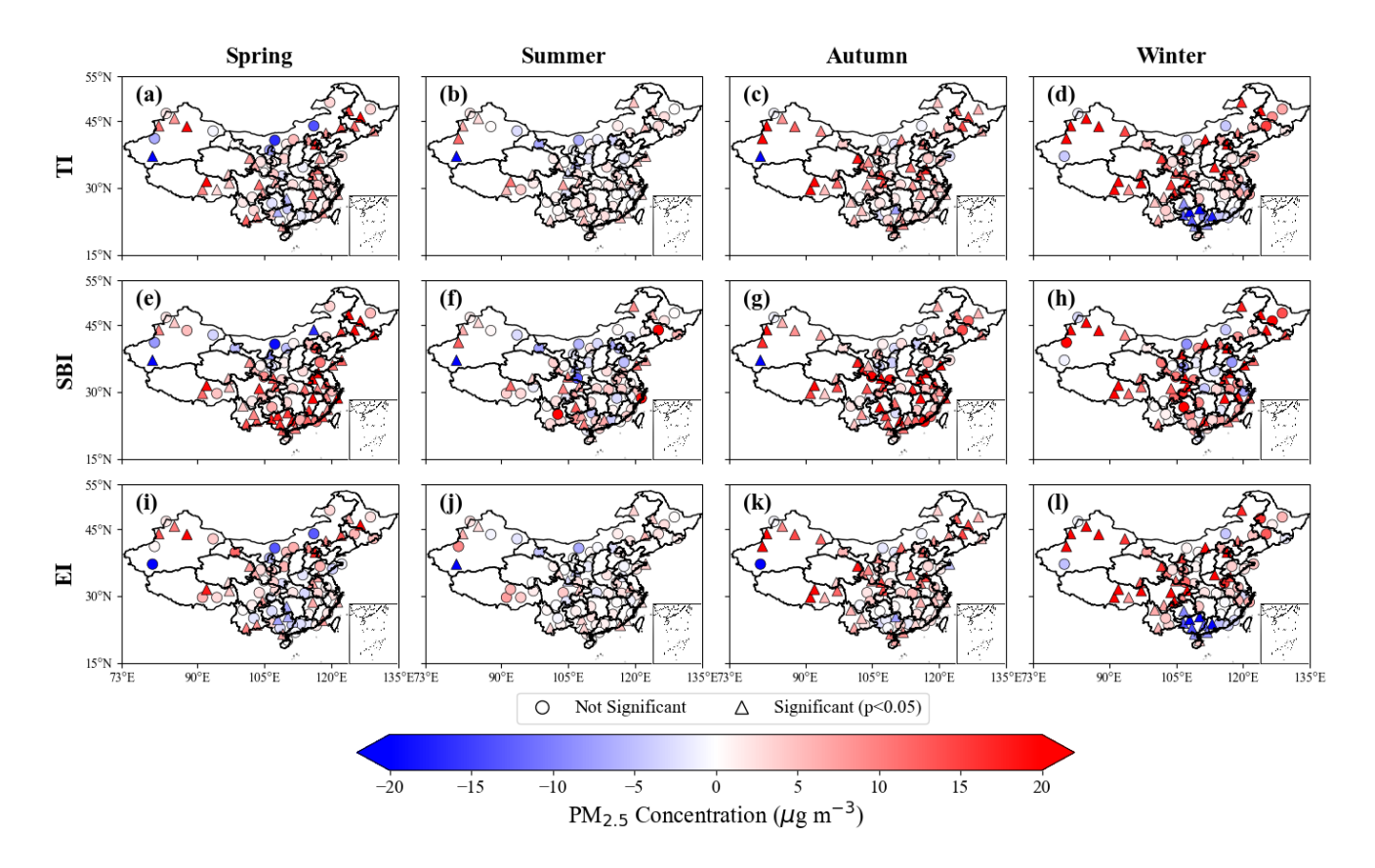


Fig S8. Distribution of PM_{2.5} concentration differences with and without temperature inversion at BJT 08:00.

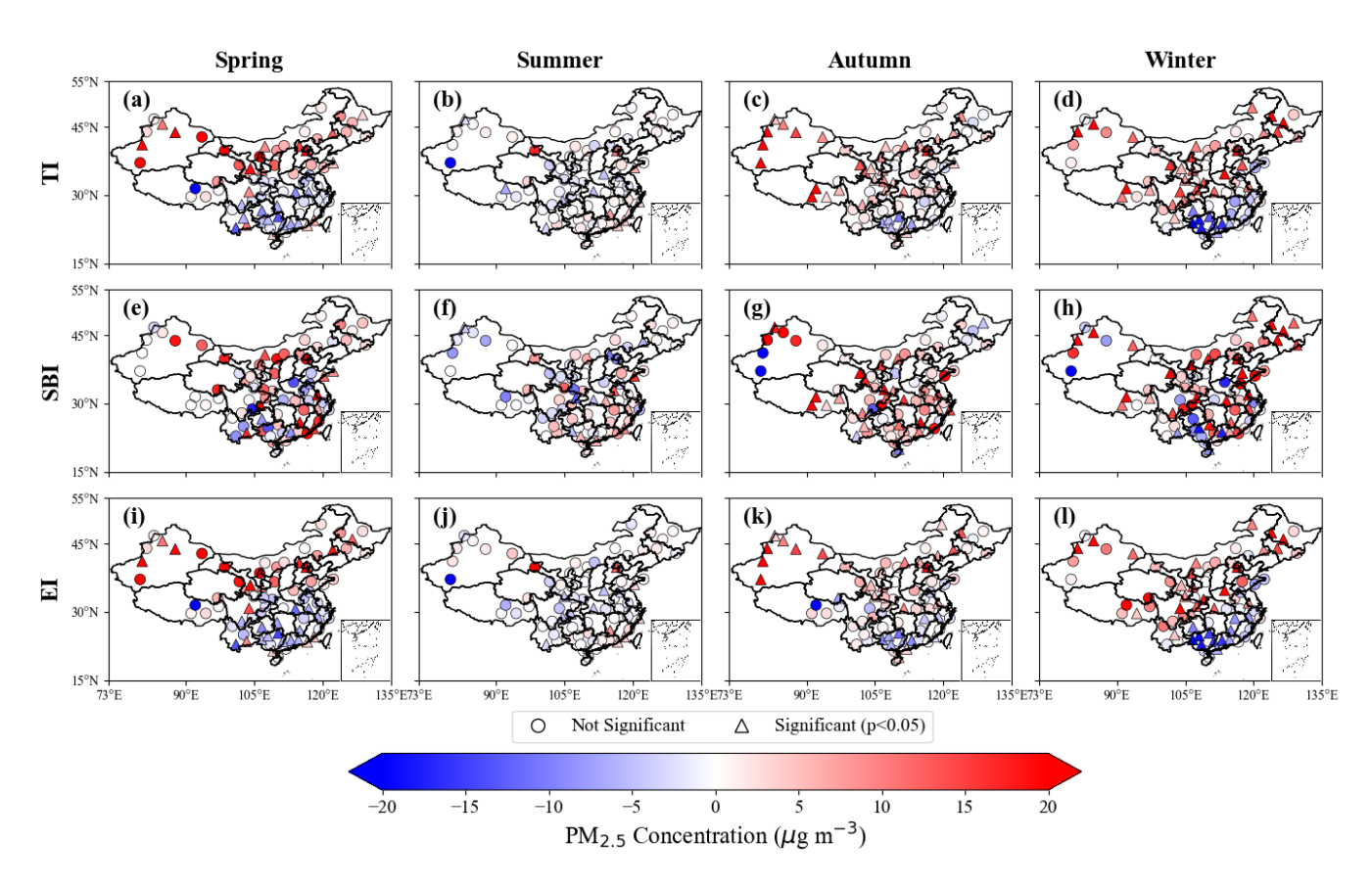


Fig S9. Distribution of PM_{2.5} concentration differences with and without temperature inversion at BJT 20:00.

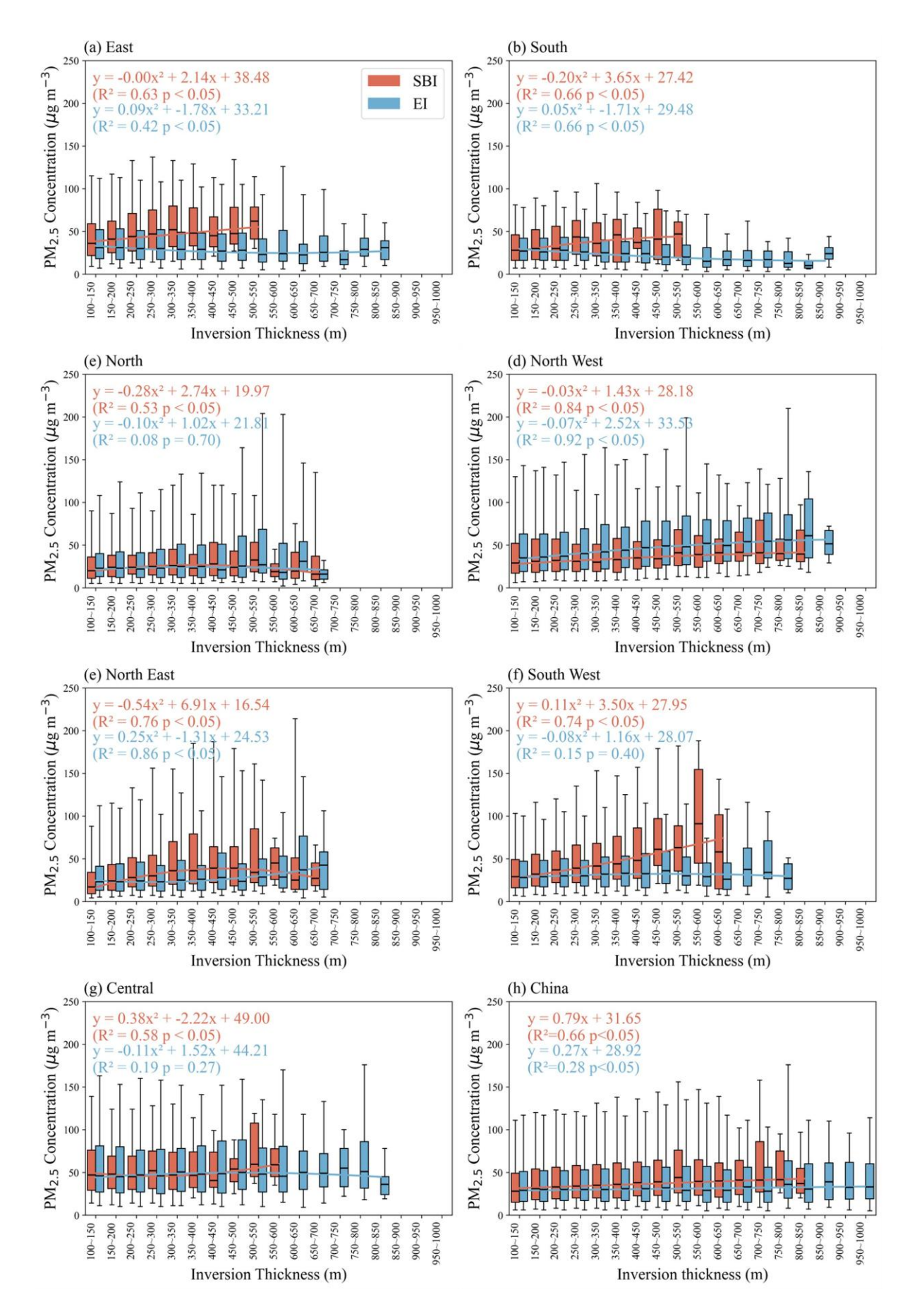


Fig. S10 Fitting relationship between inversion thickness and PM_{2.5} concentration across seven regions of China from 2016 to 2021. The ends of the boxes, the ends of the bars, and the short line across each box represent the 25th and 75th percentiles, the 5th and 95th percentiles, and the median, respectively. Each strength interval contains a sample size \geq 10.